Chinese Chemical Letters 35 (2024) 108885

Contents lists available at ScienceDirect

Chinese Chemical Letters

journal homepage: www.elsevier.com/locate/cclet

Utilization of hydralazine as a reactive matrix for enhanced detection and on-MALDI-target derivatization of saccharides

Dan Ouyang[a,1], Huan Huang[a,1], Yanting He[b], Jiajing Chen[a], Jiali Lin[a], Zhuling Chen[a], Zongwei Cai[c], Zian Lin[a,*]

[a] Ministry of Education Key Laboratory of Analytical Science for Food Safety and Biology, Fujian Provincial Key Laboratory of Analysis and Detection Technology for Food Safety, College of Chemistry, Fuzhou University, Fuzhou 350108, China
[b] School of Pharmacy, Bengbu Medical University, Bengbu 233000, China
[c] Partner State Key Laboratory of Environmental and Biological Analysis, Department of Chemistry, Hong Kong Baptist University, Hong Kong, China

ARTICLE INFO

Article history:
Received 28 February 2023
Revised 31 July 2023
Accepted 1 August 2023
Available online 4 August 2023

Keywords:
Hydralazine
Reactive matrix
On-MALDI-target derivatization
Saccharides

ABSTRACT

Saccharides are a sort of ubiquitous and vital molecules within the whole life. However, the application of saccharides analysis with matrix-assisted laser desorption/ionization mass spectrometry (MALDI-MS) is restricted by their low ionization efficiency and the instability of the sialic acid fraction. Derivatization strategy based on nonreductive amination provides a good solution, however, this is often time consuming and may result in sample loss due to removal of excessive derivatization reagents. Herein, hydralazine (HZN) was utilized as a reactive matrix for labeling reducing saccharides directly on MALDI target which eliminated tedious sample preparation and avoided sample loss. After optimization, effective and reproducible on-MALDI-target derivatization of neutral and acidic saccharides was achieved in both positive and negative modes. Compared with 2,5-dihydroxybenzoic acid (DHB) and 9-aminoacridine (9-AA), HZN improved the detection sensitivity of reducing saccharides and provided more abundant fragment ions in MS/MS analysis. Moreover, 26 kinds of neutral glycans and 5 kinds of sialic glycans were identified from ovalbumin (OVA) and bovine fetuin, respectively. Combined with the statistical models, this strategy could be used to distinguish and predict samples of 6 brands of beer, and discriminate 2 kinds of beer fermentation modes. In addition, HZN was applied for quantitative analysis of glucose in urine samples, and the obtained urine glucose concentrations of diabetic patients were consistent with the clinical test results, showing the potential of qualitative and quantitative analysis of reducing saccharides in complex samples.

Saccharides are an indispensable intermediate metabolite for life activities as a major source of energy and information, which are also essential for many food materials or products [1]. In addition, glycosylation, one of the most prevalent post-translational modifications of proteins in living organisms, is closely linked to cellular interactions, signaling and the development of disease [2,3]. However, saccharides are usually in low abundance in complex samples and lack of UV absorbing groups, creating major challenges in direct analysis [4]. Therefore, it is desirable to construct sensitive and selective tool for analysis of saccharides accurately and rapidly.

Matrix-assisted laser desorption/ionization mass spectrometry (MALDI-MS), an increasingly significant technique for biomolecular analysis owing to its soft ionization, high throughput, and good salt tolerance, has been extensively applied in the field of saccharide profile [5,6]. Despite the considerable success, the ionization efficiency of native saccharide is poor due to the strong hydrophilicity, low proton affinity from aldehydes/ketones and multiple hydroxyl groups [7,8]. Additionally, sialic acid residues are unstable and easily dissociated, and saccharide with low molecular weight easily suppressed by interferences, thus direct analysis of saccharide by MALDI-MS generally has low sensitivity [9].

To address these issues, a series of chemical derivatization strategies have emerged to improve detection sensitivity of saccharide in MALDI-MS, such as reductive amination, amidation and permethylation [10–13]. Nonetheless, conventional chemical derivatization usually requires the removal of excess reagents which possibly leading to sample loss, making sample preparation tedious and time-consuming [14]. Recently, great efforts are devoted to streamline the derivatization of saccharide in MALDI-MS analy-

* Corresponding author.
E-mail address: zianlin@fzu.edu.cn (Z. Lin).
[1] These authors contributed equally to this work.

https://doi.org/10.1016/j.cclet.2023.108885
1001-8417/

sis [15]. One that received a lot of attention is non-reducing amination, where these labeling reagents contain amino/hydrazine groups and can react with aldehydes/ketones into reduced saccharide on MALDI plate *via* a Schiff base dehydration reaction. The derivatization occurs during the MALDI-MS analysis and the excessive labeling reagent is used directly as a matrix, thus eliminating the additional reducing steps. 3-Aminoquinoline (3-AQ) [16], hydrazinylnico-tinic acid (HYNIC) [17,18], 2-phenyl-3-(*p*-aminophenyl)acrylonitrile (PAPAN) [19], 2-hydrazinoquinoline (2-HQ) [20] and 2-aminobenzoic acid (2-AA) [4] were all severed as reactive matrices in MALDI-MS, minimizing sample preparation time and avoiding potential sample loss. Some studies have combined such derivatization reagents with traditional organic matrices to assist the desorption ionization of analyte [21–24], such as 3-AQ/*p*-coumaric acid (CA) and 2-hydrazinopyrimidine/2,5-dihydroxybenzoic acid (2-HPM/DHB). Nevertheless, there are very few compounds with such special properties. Therefore, it is still challenging to develop reactive matrices for the direct and specific detection of saccharide from complex samples.

Hydralazine (HZN) has been reported to be used as a dual-mode broad-spectrum matrix for universal application that cover small to macromolecules (including small metabolites, lipids and proteins) [25]. On the other hand, with two electron-absorbing imine nitrogen, HZN can further enhance the reactivity of the hydrazine group towards the reducing end of the saccharide, and the phthalazine structure helps to enhance the MALDI-MS signal of analyte [26]. Hence, we proposed and explored HZN as a reactive matrix in this work to facilitate the analysis of saccharides and to improve ionization efficiency and ionization stability. Consequently, the application of HZN as a MALDI matrix is further broadened, not only for lipid, small molecule and protein, but also for the sensitive detection of neutral and acidic saccharide in MS and MS/MS analysis, and identification of complex glycans from OVA and bovine fetuin by optimizing the reaction conditions. In addition, based on the good reproducibility of HZN, it was successfully applied to the differentiation of beer samples and the quantitative analysis of glucose in diabetic urine samples.

HZN was prepared by alkalinizing HZN·HCl with ammonia, extracting with chloroform and then blowing to dryness with nitrogen in a yield of 58.9%. The reducing saccharide has a cyclic hemiacetal/ketone structure, which can be transformed into an open chain structure. Therefore, hydrazone can be formed *via* the reaction between the hydrazine of HZN and the carbonyl of reducing saccharide (Scheme 1).

In order to exploit the best performance of the reactive matrix, 0.1 mmol/L maltohexaose was selected as a model saccharide. The solvent type, along with matrix concentration, acid type and concentration, reaction temperature and time was optimized in detail to obtain the favorite derivatization efficiency and MS response.

Firstly, the solvent type was optimized. As shown in Fig. 1A, the derivatization efficiencies obtained in the positive mode were 46.06%, 74.82%, 62.58%, and 30.63% with methanol, ethanol, water, and acetonitrile as solvents, respectively. In addition, the peaks of maltohexaose with ethanol as solvent was stronger than that of methanol, water, and acetonitrile. It is noteworthy that no matrixes-related peaks and analyte peaks were observed with acetone, but numerous interfering peaks appeared (Fig. S1A in Supporting information). In the UV-vis absorption spectra of the five solutions (Fig. S1B in Supporting information), the peak with acetone solvent was greatly changed, presuming that HZN might have reacted with acetone to form a hydrazone. Therefore, we chose ethanol as the solvent of HZN.

As is known to all, the concentration of matrix plays a crucial role in the detection sensitivity of MALDI-MS. As presented in Fig. S2 (Supporting information), the MS response of analyte increased significantly with the increasing matrix concentrations.

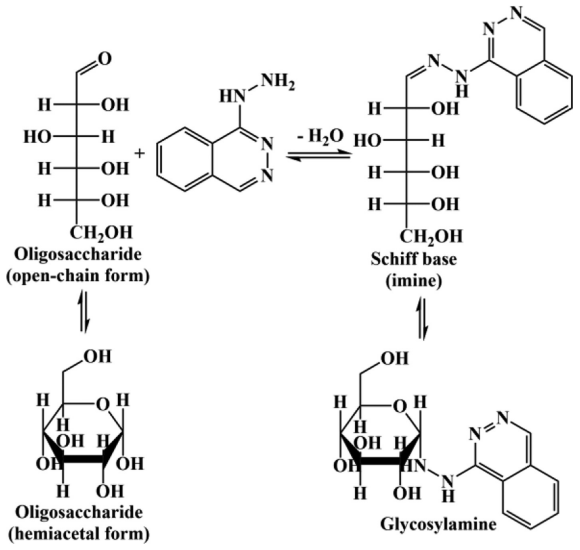

Scheme 1. Formation of Schiff bases between HZN and reducing saccharide.

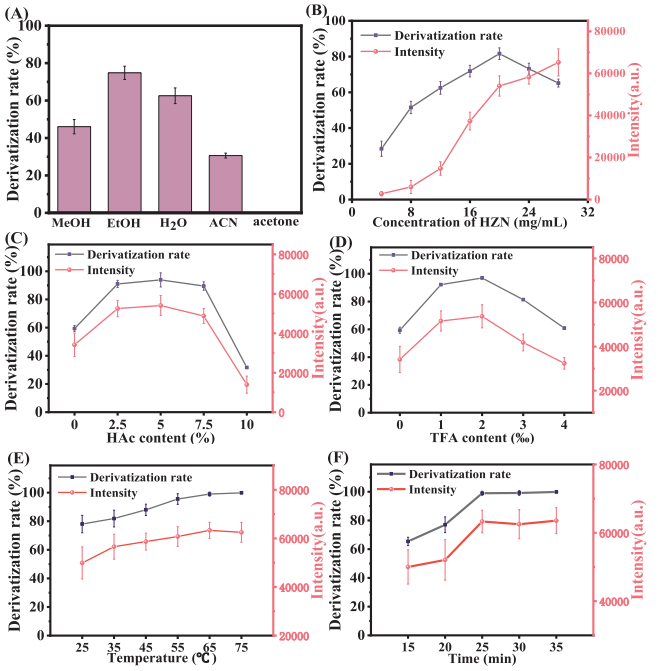

Fig. 1. Effects of on-MALDI-target derivatization efficiency of maltohexaose. (A) solvents, (B) concentration of HZN, (C) concentration of HAc, (D) concentration of TFA, (E) reaction temperature, and (F) reaction time.

The derivatization efficiency and total intensity of maltohexaose were shown in Fig. 1B, where the derivatization efficiency increased from 28.43% to 81.62% as the matrix concentration increased from 4 mg/mL to 20 mg/mL. Notably, the derivatization efficiency decreased slightly when the concentration of HZN was over 20 mg/mL. This might because of the thicker crystals formed by too high matrix concentration, which slowed the dehydration process in the reaction with the analyte, therefore affecting the derivatization efficiency. Finally, 20 mg/mL HZN was selected for the following detection.

Since the Schiff base reaction is performed in a weakly acidic environment, two commonly used acids including acetic acid (HAc) and trifluoroacetic acid (TFA) were selected for the optimization of acid type and concentration. We first investigated the effect of HAc concentration (Fig. 1C and Fig. S3 in Supporting information).

The derivatization efficiency was only 59.35% without HAc, and increased to 93.87% when the HAc concentration was increased to 5%, accompanied by an increase in MS response. On the other hand, the derivatization efficiency started to decrease when the HAc concentration continued to increase. Notably, the sample spot was still in the liquid state with 15% HAc, indicating that too high acid concentration would promote the reverse of the non-reducing amination. Continue to react the sample spot with 15% HAc for 2 h, an almost complete derivatization was obtained. This suggested that by extending the reaction time, satisfactory derivatization results could still be obtained with the evaporation of the liquid, further demonstrating that too high acid concentration hindered the non-reductive amination. For the impact of TFA concentration, the overall trend was similar to HAc (Fig. 1D). The highest derivatization efficiency (96.98%) was obtained with 0.2% TFA, while it began to decrease as the TFA concentration continued to increase. Moreover, the pH value of HZN ethanol solution (20 mg/mL) was 6.7∼7.2, and those corresponding solution containing 0.2% TFA and 5% HAc were 4.8∼5.4, implying that the derivatization efficiency of neutral saccharides was independent of the type of acid, but only related to the pH value.

For acidic saccharides, it is suitable for detection in negative mode because the H^+ in the carboxyl group is easy to dissociate. The detection of sialic acid was performed in negative mode using HZN solutions containing 5% HAc and 0.2% TFA, respectively. The results exhibited that a poor MS response of the matrix-related peak ($[HZN\text{-}H]^-$) with many spurious peaks was shown with TFA, and the intensity of the analyte was much lower than that of the analyte with HAc (Fig. S4 in Supporting information). It can be concluded that the strong acid would inhibit the dissociation of H^+ from acidic saccharides, resulting in a much lower MS response in negative mode. Hence, we chose 5% HAc for further optimization.

Worth of mention are also reaction temperature and reaction time. The derivatization efficiency and the total intensity of the analyte increased with the reaction temperature raised. After the temperature reached 65 °C, further increasing the temperature no longer had a significant effect on the detection (Fig. 1E). As for the reaction time, a longer reaction time ensured complete derivatization. In addition, the best derivatization efficiency was calculated to be 99.85% when the reaction time reached more than 30 min (Fig. 1F). In summary, we selected 20 mg/mL HZN ethanol solution containing 5% HAc and reacted with saccharides at 65 °C for 35 min before detection.

Non-reducing saccharide lacks free hemiacetal/ketone hydroxyl groups and cannot be derivatized with HZN. Firstly, raffinose and nistose trihydrate were selected to examine the ability of HZN as a common matrix. As shown in Fig. S5 (Supporting information), HZN was able to obtain comparable analytical results with DHB in the analysis of non-reducing saccharide.

Next, the feasibility of HZN for the detection of saccharides with low molecular weight (mono- and disaccharides) was evaluated in neutral reducing saccharide detection. The MS response of these saccharides was significantly increased after HZN derivatization compared to DHB in positive mode (Fig. 2A and Fig. S6A in Supporting information). Consequently, maltotriose, maltotetraose and maltopentaose were further detected. Similarly, the MS response of the three saccharides was significantly increased after HZN derivatization compared to DHB (Fig. 2B and Fig. S6B in Supporting information).

Because of the preferential dissociation of sialic acid residues and the negative charge of multiple carboxyl groups, it is difficult to detect sialylated glycans even in negative mode of MALDI-MS. To estimate the feasibility of HZN to analyze acidic reducing saccharide in negative mode, sialic acid and disialyloctasaccharide were used as model analytes. As observed in Fig. S7 (Supporting information), when 9-AA was adopted as the matrix, the background interference was serious, and the signal to noise (S/N) of the $[M\text{-}H]^-$ of sialic acid (*m/z* 308.098) was only 33. As for HZN, however, the S/N of the $[M+HZN\text{-}H_2O\text{-}H]^-$ peak (*m/z* 450.162) increased to 673 (Fig. 2C). In the detection of disialyloctasaccharide (Fig. 2D), the $[M+HZN\text{-}H_2O+Na\text{-}2H]^-$ (*m/z* 2184.095) with an S/N of 415 was identified, which was much better than $[M+Na\text{-}2H]^-$ (*m/z* 2040.962) detected with 9-AA. The aforementioned results revealed that HZN was an effective reactive matrix for the derivatization of reducing saccharide, which could enhance the detection sensitivity of neutral and acidic reducing saccharide.

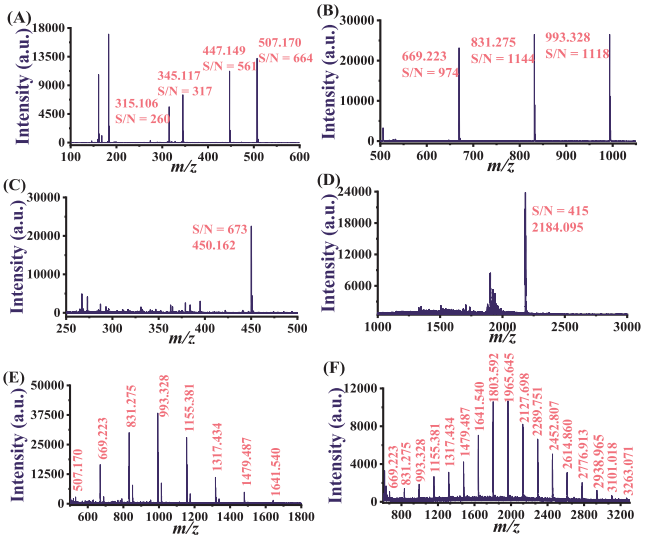

Fig. 2. Mass spectra using HZN as reactive matrix of (A) mixture of xylose, glucose, xylobiose and lactose, (B) mixture of maltotriose, maltotetraose and maltopentaose, (C) sialic acid, (D) disialyloctasaccharide, (E) glucan 1K, and (F) glucan 2K.

To further investigate the ability of the HZN-assisted on-MALDI-target derivatization method to characterize the polymers, the glucan 1K and 2K were chosen to be studied. The molecular weight distributions showed a Gaussian distribution with a spacing of 162 Da, corresponding to the glucose residue (Figs. 2E, F and Fig. S8 in Supporting information). After derivatization, all glucan with different degrees of polymerization were effectively labeled and converted into HZN-labeled Na^+ adducts with a mass increment of 162 Da, which displayed more analyte-related peaks and higher signal intensity compared to DHB. Taken together, HZN could be used both as a common matrix and as a reactive matrix to analyze different saccharides.

Good reproducibility is essential for quantitative analysis. The cocrystallization between matrix and analyte have an effect on the reproducibility to some extent. Fig. S9 (Supporting information) showed that the cocrystallization by HZN and analyte was more uniform and denser than that of DHB and 9-AA. Furthermore, the relative standard deviation (RSD) of shot-to-shot with HZN was 4.9%-6.0%, with DHB was 48.9% (sometimes no glucose peak was detected with DHB), and with 9-AA was 20.7%-31.9%. In addition, the RSD of dot-to-dot of HZN was 6.5%-7.9%, with DHB was 60.2%, and with 9-AA was 29.8%-38.4% (Table S1 in Supporting information). The above results revealed that HZN had superior reproducibility, therefore improving the reliability of the analytical results.

MS/MS is a key method for high-throughput identification and characterization of glycans. Glycosidic bond cleavage provides structural information on the sequence of monosaccharide, while cross-ring cleavage is used to determine how the glycans are linked. Hereto, maltohexaose was used to explore its bond-breaking form in MS/MS. The fragmentation peaks were defined

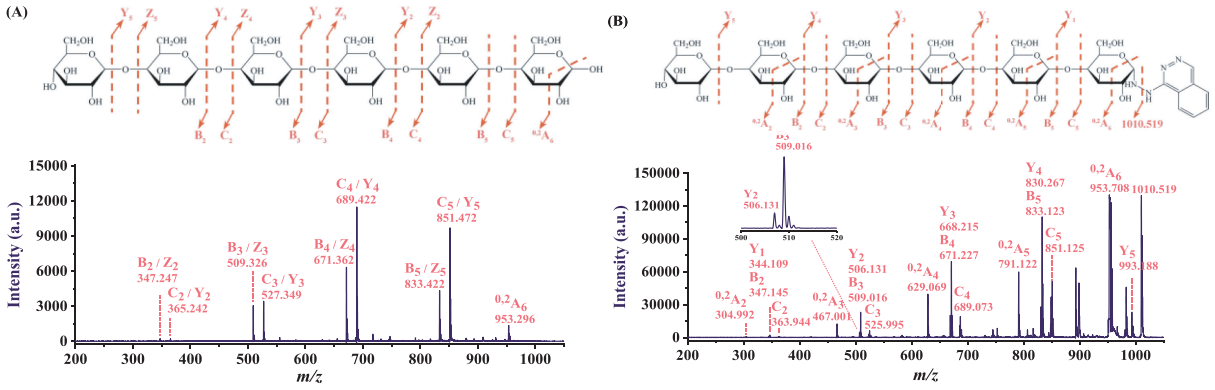

Fig. 3. MS/MS spectra of maltohexaose. (A) DHB as matrix (B) HZN as matrix.

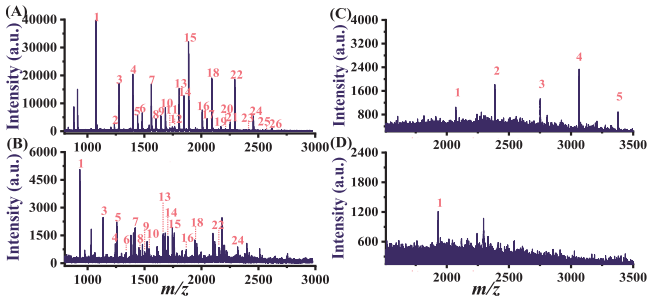

Fig. 4. Mass spectra of N-glycans from OVA in positive mode with (A) HZN and (B) DHB. Mass spectra of N-glycans from bovine fetuin in negative mode with (C) HZN and (D) 9-AA.

according to the nomenclature proposed by Domon and Costello [27]. It is difficult to respectively distinguish the cleavage product (B/C fragment) of non-reducing end from the reducing end (Z/Y fragment), because both reducing and non-reducing cleavage products are capable of being charged during fragmentation. As illustrated in Fig. 3A, only a weak $^{0,2}A_6$ cross-ring cleavage peak was observed at *m/z* 953.296 with DHB as matrix, accompanied by many other fragmentation peaks with the very similar *m/z*, thus complicating the characterization of glycans.

After derivatization with HZN (Fig. 3B), the C- and Y-type as well as the Y- and B-type ions of maltohexaose could be easily and better distinguished. In addition, the $^{0,2}A_6$ cross-ring cleavage ion (*m/z* 953.708) with significantly enhanced signal indicated the formation of closed-ring glycosylamine and the immediate loss of the HZN label. A series of cross-ring cleavage ions generated by internal cleavage obtained from type $^{0,2}A_6$ ions such as $^{0,2}A_2$, $^{0,2}A_3$, $^{0,2}A_4$ and $^{0,2}A_5$ were well observed in the figure, providing important information for revealing the type of linkage between monosaccharides [24]. It can be concluded that HZN derivatization could provide enhanced signal and a richer abundance of easily distinguishable fragment ions in MALDI MS/MS analysis, thus facilitating the structure determination of glycans.

Glycan profiling in glycoproteins plays an important role for biomarker discovery or antibody evaluation [28]. OVA was selected to explore the feasibility of on-MALDI-target derivatization with HZN in neutral glycan analysis. The glycans were released from OVA by the PNGase F, and analyzed directly without any pre-purification process. As shown in Fig. 4A, a total of 26 HZN-labeled N-glycans were detected using HZN as reactive matrix. As a control, however, only 16 N-glycans were detected with a lower signal using DHB matrix (Fig. 4B), and the detail information of all glycans was presented in Table S2 (Supporting information) [29,20]. In addition, more N-glycans released from OVA were detedcted compared with previous reported reactive matrixes (Table S3 in Supporting information) [19,20,30–32]. The above results suggested that the HZN matrix not only improved the detection sensitivity of the glycans, but also had high tolerance to protein and buffer interference.

It is usually difficult to detect multi-sialylated glycans in MALDI-MS because of the instability and easy dissociation of sialic acid [33]. In this case, bovine fetuin was chosen as a model glycoprotein for the detection of salivated glycans, whose N-glycan pool was composed of a low-abundance high mannose neutral glycan (M5) and five complexes salivated glycans (A2G2S1, A2G2S2, A2G3S2, A3G3S3, A3G3S4) [4]. Following the release of glycans from bovine fetuin by PNGase F, HZN-labeled sialylated glycans were detected in negative mode. All five types of sialylated glycans were detected as $[M+HZN-H_2O+(n-1)Na-nH]^-$ (n: number of sialic acid residues in the glycan) in Fig. 4C. In turn, only one monosialylated N-glycan was detected as $[M-H]^-$ with 9-AA (Fig. 4D). The detail information of all sialylated glycans was shown in Table S4 (Supporting information) [20].

Saccharides are essential components of many plants and are important substrates for the fermentation process [34]. Beer is mainly made through malt treatment, saccharification and fermentation. The evaluation of saccharides during the brewing process is crucial, as any change in the saccharide distribution may affect the sensory characteristics of the beer [35]. Here, six brands of beer (details shown in Table S5 in Supporting information) were selected and diluted 50 times each. After on-MALDI-target derivatization of HZN, fingerprint profiles of saccharides in beer were obtained (Fig. S10 in Supporting information), in which glucan with polymerization degrees 2%-20% were identified (Table S6 in Supporting information). For each brand of beer, 11 samples were analyzed, with 80% of the samples randomly selected as the training set and 20% of the samples selected as the prediction set. The training set was normalized and subjected to principal component analysis (PCA). As depicted in Fig. 5A, the six brands were well differentiated. Subsequently, the PCA-Class model was used to establish screening criteria based on the training set of each brand sample, so as to determine the different brands. Next, the prediction set was employed to verify the discriminative predictive ability of the model. As a result, all six prediction sets were classified into the 95% confidence intervals of their respective models. As shown in Fig. 5B, this indicted that the method was effective in differentiating the beer brands without misclassification.

In addition, beer could be classified by its fermentation mode including top fermentation (namely Ale) and bottom fermentation (namely Lager) [36]. Therefore, the Ale and Lager group were classified by orthogonal partial least squares discriminant analysis (OPLS-DA) (Fig. 5C), elucidating differences in the fingerprint profiles of beer from two fermentation methods ($R^2Y(cum) = 0.867$,

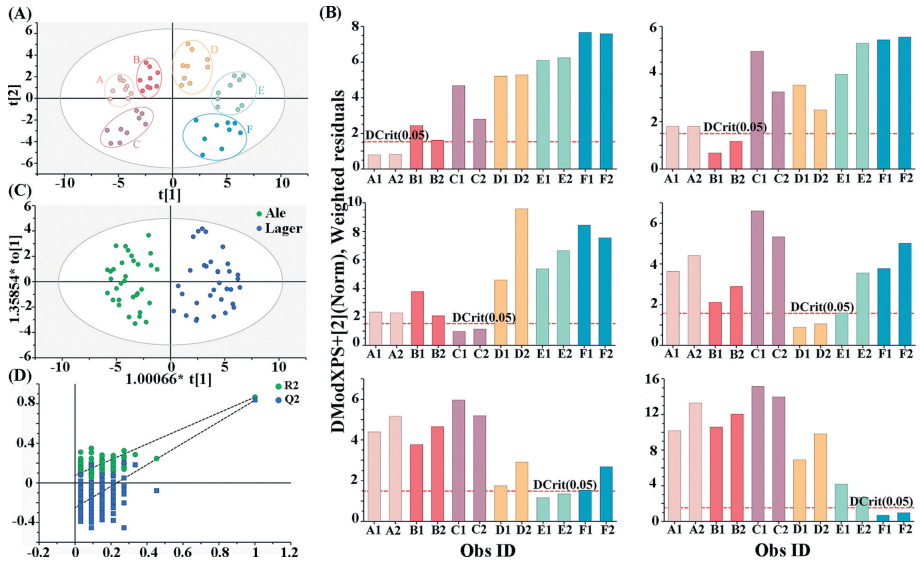

Fig. 5. (A) The PCA score plots of the training set for the six brand beers. (B) Categorization results of prediction set for the six brand beers (the six different colored bars represented six brand beers. A: Schwarzer Herzog; B: EWEN; C: MoliFood; D: Snow; E: SEDRIN; F: Budweiser). (C) OPLS-DA score plots and (D) the Permutations Plot of 33 Ale and 33 Lager.

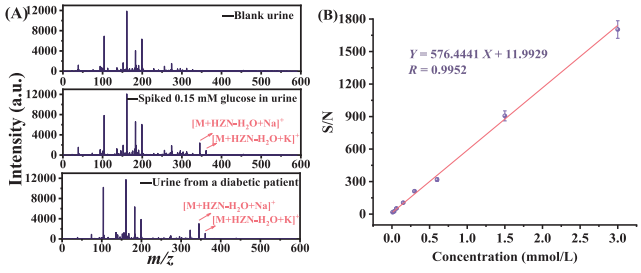

Fig. 6. (A) Analysis of glucose in urine. (B) The standard curve for glucose in spiked urine.

Q^2(cum) = 0.835). Furthermore, the results of 200 permutations in Fig. 5D reflected that the model was reliable.

Diabetes is one of the chronic diseases that have a large impact on human health, and the quantitative detection of glucose in urine can be considered as one of the indicators for the diagnosis and long-term monitoring of diabetic patients. The analysis of glucose in urine samples was illustrated in Fig. 6A, glucose was not detected in blank urine, while the glucose signal of the spiked urine and urine of diabetes were clearly observed. To verify the quantitative detection ability of the method, urine samples were spiked with different concentration of glucose (final concentrations of 0.01~3 mmol/L) and a standard curve was established by the concentrations *versus* the sum of S/N of $[M+HZN-H_2O+Na]^+$ and $[M+HZN-H_2O+K]^+$, achieving a good correlation coefficient of 0.9952 (Fig. 6B). The limit of detection (LOD) of glucose in spiked urine was 2 μmol/L (S/N = 3). Encouraged by the good performance mentioned above, the established method was applied to analysis of urine samples from diabetic patients, and the results were consistent with that of the clinical semi-quantitative assay (Table S7 in Supporting information).

In summary, an effective dual-mode MALDI-MS approach based on HZN as a reactive matrix for reducing saccharide analysis was developed, which achieved efficient and reproducible on-MALDI-target derivatization of neutral and acidic saccharides by optimizing the reaction conditions. It not only improved the detection sensitivity of saccharide, but also provided more abundant fragment ions in MS/MS. Due to the selective reaction of HZN with the reducing end of the saccharide, which effectively reduced the interference from the matrix, the approach could be used for the identification of complex glycans from OVA and bovine fetuin. Moreover, the differentiation and prediction of different beer samples, as well as the quantification of glucose in urine samples were successfully achieved. Overall, this study further expands the application of HZN, which acts not only as a broad-spectrum matrix, but promises to provide an efficient approach for saccharide analysis with the potential to be extended to more other applications (*e.g.*, glycomics).

Declaration of competing interest

The authors declare that they have no known competing financial interests or personal relationships that could have appeared to influence the work reported in this paper.

Acknowledgments

This project was supported by a grant from the National Natural Science Foundation of China (Nos. 22274021, 21974021 and 22036001), the Natural Science Foundation of Fujian Province (No. 2022J01535) and the Major Project of Science and Technology of Fujian Province (No. 2020HZ06006).

Supplementary materials

Supplementary material associated with this article can be found, in the online version, at doi:10.1016/j.cclet.2023.108885.

References

[1] J. Wang, J. Zhao, S. Nie, et al., Food Hydrocolloids 124 (2022) 107237.
[2] M.W. Patabandige, L.D. Pfeifer, H.T. Nguyen, et al., Mass Spectrom. Rev. 41 (2022) 901–921.
[3] K. Ohtsubo, J. Marth, Cell 126 (2001) 855–867.
[4] X.L. Hronowski, Y. Wang, Z. Sosic, et al., Anal. Chem. 92 (2020) 10252–10256.
[5] D.J. Harvey, Mass Spectrom. Rev. 40 (2021) 408–565.
[6] D. Ropartz, P.E. Bodet, C. Przybylski, et al., Commun. Mass Spectrom. 25 (2011) 2059–2070.
[7] H. Zhang, X. Shi, N.Q. Vu, et al., Anal. Chem. 92 (2020) 13361–13368.
[8] C.L. Wu, C.C. Wang, Y.H. Lai, et al., Anal. Chem. 85 (2013) 3836–3841.
[9] T. Nishikaze, Proc. Jpn. Acad. Ser. B 95 (2019) 523–537.
[10] L. Yang, Y. Peng, J. Jiao, et al., Anal. Chem. 89 (2017) 7470–7476.

[11] L. Wang, L. Yang, Y. Zhang, et al., Anal. Chim. Acta 1104 (2020) 87–94.
[12] Y. Cai, J. Jiao, Z. Bin, et al., Chem. Commun. 51 (2015) 772–775.
[13] S.Y. Yu, S.W. Wu, K.H. Khoo, Glycoconjugate J. 23 (2006) 355–369.
[14] S.I. Snovida, V.C. Chen, H. Perreault, Anal. Chem. 78 (2006) 8561–8568.
[15] T. Nishikaze, Mass Spectrom. 6 (2017) A0060.
[16] M. Rohmer, B. Meyer, M. Mank, et al., Anal. Chem. 82 (2010) 3719–3726.
[17] J. Jiao, Y. Zhang, P. Yang, et al., Analyst 140 (2015) 156–161.
[18] J. Jiao, L. Yang, Y. Zhang, et al., Analyst 140 (2015) 5475–5480.
[19] L. Ling, C. Xiao, Y. Ma, et al., Anal. Chem. 91 (2019) 8801–8807.
[20] X. Lin, C. Xiao, L. Ling, et al., Talanta 235 (2021) 122792.
[21] K. Kaneshiro, Y. Fukuyama, S. Iwamoto, et al., Anal. Chem. 83 (2011) 3663–3667.
[22] K. Kaneshiro, M. Watanabe, K. Terasawa, et al., Anal. Chem. 84 (2012) 7146–7151.
[23] Y. Fukuyama, N. Funakoshi, K. Takeyama, et al., Anal. Chem. 86 (2014) 1937–1942.
[24] K. Jiang, A. Aloor, J. Qu, et al., Anal. Bioanal. Chem. 409 (2017) 421–429.
[25] W. Tang, A. Gordon, F. Wang, et al., Anal. Chem. 93 (2021) 9083–9093.
[26] R. Breslow, E. McNelis, J. Am. Chem. Soc. 81 (1959) 3080–3082.
[27] B. Domon, C.E. Costello, Glycoconjugate J. 5 (1988) 397–409.
[28] O. Aizpurua-Olaizola, J. Sastre Toraño, J.M. Falcon-Perez, et al., Trends Analyt. Chem. 100 (2018) 7–14.
[29] X. Lin, C. Xiao, L. Ling, L. Guo, X. Guo, Talanta 235 (2021) 122792.
[30] L. Ling, S. Yu, C. Ding, Analyst 146 (2021) 6840–6845.
[31] Y. Cai, Y. Zhang, P. Yang, et al., Analyst 138 (2013) 6270–6276.
[32] X. Yang, J. Gan, H. Yuan, et al., Int. J. Mass Spectrom. 417 (2017) 76–82.
[33] S. Holst, B. Heijs, N. De. Haan, et al., Anal. Chem. 88 (2016) 5904–5913.
[34] P. Mauri, M. Minoggio, P. Simonetti, et al., Rapid Commun. Mass Spectrom. 16 (2002) 743–748.
[35] O. Šedo, I. Márová, Z. Zdráhal, Food Chem. 135 (2012) 473–478.
[36] R. Castro, A.B. Díaz, E. Durán-Guerrero, et al., J. Food Compos. Anal. 106 (2022) 104278.